SLAC-PUB-13082
January 2008

Evidence for Color Transparency and Direct Hadron Production at RHIC *

Stanley J. Brodsky
Stanford Linear Accelerator Center, Stanford University, Stanford, California 94309

The QCD color transparency of higher-twist contributions to the inclusive hadroproduction cross section, where the trigger proton is produced directly in a short-distance subprocess, can explain several remarkable features of high-p_T proton production in heavy ion collisions which have recently been observed at RHIC: (a) the anomalous increase of the $p \to \pi$ ratio with centrality (b): the more rapid power-law fall-off at fixed $x_T = 2p_T/\sqrt{s}$ of the charged particle production cross section in high centrality nuclear collisions, and (c): the anomalous decrease of the number of same-side hadrons produced in association with a proton trigger as the centrality increases. These phenomena illustrate how heavy ion collisions can provide sensitive tools for interpreting and testing fundamental properties of QCD.

Submitted to RHIC News

*Work supported in part by the U.S. Department of Energy under contracts DE–AC02–76SF00515

One of the most surprising results observed at RHIC is the behavior of the ratio of protons to pions produced at large transverse momenta in heavy ion collisions. Since the inelastic cross section of the proton is significantly larger than that of the pion, one expects that a proton would lose more energy and be more absorbed than a pion as it traverses the nuclear medium; however, the PHENIX [1] and STAR experiments [2] observe just the opposite. As shown in Figure 1, the p/π ratio at $p_T \sim 4$ GeV/c increases with the centrality of the heavy ion collision as measured by the total number of particles produced. Even more remarkably, the number of same-side hadrons produced in correlation with a high p_T proton trigger *decreases* with increasing centrality in heavy ion collisions which have very large numbers of produced particles [3, 4]. See Figure 2. These anomalous differences between the nuclear dependence of pion and proton production cannot be easily explained in terms of the standard perturbative QCD picture of Figure 3 where quarks or gluons scatter at large transverse momentum and produce hadrons through their jet fragmentation.

The most direct test of pQCD in hard hadronic collisions is the scaling of the inclusive cross section

$$\frac{d\sigma}{d^3p/E}(pp \to HX) = \frac{F(x_T, \theta_{cm})}{p_T^n}$$

at fixed $x_T = 2p_T/\sqrt{s}$. In the original parton model [5] the power fall-off is simply $n = 4$ since the underlying $qq \to qq$ subprocess amplitude for point-like partons is scale invariant, and there is no dimensionful parameter in the theory. The Bjorken scaling of the deep inelastic lepton cross section $\ell p \to \ell' X$ is based on the same scale-invariance principle. In a full perturbative QCD analysis based on 2-to-2 quark and gluon subprocesses, the scale-invariance of the inclusive cross section is broken by the logarithmic running of the running coupling and the evolution of the structure functions and fragmentation functions. These effects increase the prediction for n to $n = 4.5 \to 5$ as illustrated in Figure 4 [6].

There have been extensive measurements of inclusive hadron production cross sections, particularly from the CERN ISR and fixed-target experiments at FermiLab. As summarized by Cronin in his 1974 review [7], the cross sections measured for $pp \to \pi X$ and $pp \to pX$ are far from scale-invariant. See Figure 5. The power fall-off at fixed x_T is consistent with the leading twist pQCD prediction $n = 4.5 \to 5$ only at the very smallest values of x_T. In fact, n is not a constant power ; it is observed to be a monotonically increasing function of x_T, reaching $n = 20$ for $pp \to pX$ at the exclusive limit $x_T \to 1$.

In the case of the RHIC collider, the shape of the inclusive cross section for pion production measured in peripheral collisions at $\sqrt{s} = 200$ GeV [8] is in general agreement with NLO leading-twist QCD expectations [9]. However, as seen in Figure 6, the scaling of the pion data at fixed x_T for $0.03 < x_T < 0.06$ shows a rising behavior of $n(x_T)$ with an average value $n \sim 6.4 \pm 0.5$ [8]. Figure 1 also shows that the proton-to-pion and antiproton to meson ratios measured in peripheral and central heavy ion collisions differ from that of quark and gluon jets in e^+e^- annihilation. [1] This breakdown of factorization also suggests that a description of the heavy ion hadroproduction data based solely on leading-twist contributions is not adequate. In contrast, as illustrated in Figure 7, the photon production cross section [10, 11] $pp \to \gamma X$ at fixed x_T scales over a large range of energies with a constant power $n \sim 5$ at $x_T < 0.04$, consistent with the leading-twist PQCD prediction based on the $gq \to q\gamma$ subprocess. The direct comparison of the $\gamma \to \pi$ ratio with theory at fixed x_T would be illuminating; if the leading twist description is correct, the ratio should be nearly scale-invariant except for small corrections from jet fragmentation and the running coupling. The choice of renormalization scale for each subprocess, including the non-Abelian couplings, can be fixed using the BLM method [12, 13], thus eliminating one source of ambiguity of the leading-twist predictions ,

The seemingly anomalous scale-breaking behavior for hadroproduction can be naturally explained if in addition to the leading twist processes, there are also contributions from "higher twist " (multiparton processes). As x_T increases, it becomes more advantageous to produce the trigger hadron directly in a semi-exclusive hard subprocess [14] such as $gq \to \pi q$ or $qq \to p\overline{q}$, since this avoids any waste of energy from jet fragmentation [15] . An example is illustrated in Figure 8. It is also more energy efficient to scatter more than one parton in the projectile, such as $q+(qq) \to q(qq)$ followed by fragmentation of the diquark to the trigger proton. In each case the penalty of the extra fall-off in p_T from hadron compositeness or the diquark correlation scale is compensated by a lesser fall-off in x_T.

Dimensional counting rules provide a simple rule-of-thumb guide for the power-law fall-off of the inclusive cross section in both p_T and $(1-x_T)$ due to a given subprocess [16]:

$$E\frac{d\sigma}{d^3p}(AB \to CX) \propto \frac{(1-x_T)^{2n_{spectator}-1}}{{p_T}^{2n_{active-4}}}$$

where n_{active} is the "twist", i.e., the number of elementary fields participating in the hard subprocess, and $n_{spectator}$ is the total number of constituents in A, B and C not participating in the hard-scattering subprocess. For example, consider $pp \to pX$. The leading-twist contribution from $qq \to qq$ has $n_{active} = 4$ and $n_{spectator} = 6$. The higher-twist subprocess $qq \to p\overline{q}$ has $n_{active} = 6$ and $n_{spectator} = 4$. This simplified model provides two distinct contributions to the inclusive cross section

$$\frac{d\sigma}{d^3p/E}(pp \to pX) = A\frac{(1-x_T)^{11}}{p_T^4} + B\frac{(1-x_T)^7}{p_T^8}$$

and $n = n(x_T)$ increases from 4 to 8 at large x_T.

Multi-parton and semi-exclusive subprocesses underly the analysis of hard exclusive processes such as deeply virtual Compton scattering, deeply virtual meson production, fixed-angle scattering, and elastic and inelastic form factors at large momentum transfer. A particularly important example for inclusive reactions is the Drell-Yan process $\pi p \to \gamma^* X$ where the direct $n_{active=5}$ higher-twist subprocess

$\pi q \to \gamma^* q$ dominates lepton pair production at high x_F, explaining the constant behavior of the cross section as a function of the parton momentum fraction and the observed dominance of longitudinally polarized virtual photons [17]. The nonperturbative wavefunction which controls the direct higher-twist process $\pi q \to \gamma^* q$ is the gauge invariant and frame-independent pion distribution amplitude [18] $\phi_\pi(x)$. The shape and normalization of hadronic distribution amplitudes can now be predicted using the AdS/QCD correspondence [19].

In a general QCD analysis of inclusive hadroproduction one needs to sum over all contributing leading and higher-twist hard subprocesses. At $x_T = 1$ the quarks in the protons must all scatter in an $n_{active} = 12, n = 20, n_{spectator} = 0$ exclusive subprocess. In each case the nominal fall-off given by counting rules will be increased by the running of the QCD coupling and either DGLAP evolution of the structure functions or ERBL evolution [18, 20] of the distribution amplitudes for the directly-interacting hadrons. Although large p_T hadron production at RHIC is most likely dominated by leading-twist QCD processes [21], higher-twist subprocesses can play a significant role, particularly in the case of proton production.

In higher-twist subprocess such as $gq \to \pi q$ $\pi q \to \gamma^* q$ or $qq \to p\overline{q}$, the wavefunction of a hadron enters directly into the amplitude. The dominant contribution comes from fluctuations of the hadronic wavefunction where the quarks in the valence Fock state are at small impact separation $b_\perp \sim 1/p_T$. Interactions with the external system is thus suppressed unless the wavelength of the exchanged gluon is comparable to the transverse size of the color singlet system; ie $k_\perp \sim p_\perp$ The small-size color-singlet configurations of the hadron can thus propagate through the nuclear medium with minimal hadronic interactions; i.e. they are *color transparent* [22].

Color transparency [23, 24] is a fundamental property of QCD as a gauge theory of hadronic interactions. A clear empirical demonstration has been given in diffractive dijet production $\pi A \to \text{jetjet} A'$ by the E791 experiment at Fermilab [25]; the forward amplitude for the diffractive production of high transverse momentum dijets is found to scale as A^α where $\alpha \simeq 1$; i.e. the diffractive dijet production amplitude is coherent on every nucleon in the nucleus. This is in dramatic contradiction to traditional Glauber theory where only nucleons on the periphery of the nucleus are effective. Color transparency predictions for quasi-elastic pion electoproduction $eA \to e'\pi^+ X$ have recently been verified at Jefferson Laboratory[26].

Color transparency was first observed by the EVA fixed target experiments [27, 28] at BNL in quasielastic large angle proton-proton scattering. The effective number of protons in the nuclear target was shown to grow with transverse momentum, as predicted by QCD. However, the interpretation of this experiment is complicated by the anomalous quenching of color transparency at $\sqrt{s} \sim 5$ GeV, in the same kinematical regime where a remarkably strong spin-spin correlation A_{NN} in transversely polarized pp scattering is observed [29]. A possible explanation [30] for the breakdown of color transparency and the anomalous spin-spin correlation is resonance production at the charm production threshold in the intermediate state for pp scattering.

Color transparency provides an appealing explanation of the anomalous p/π ratio observed at RHIC. For simplicity, let us assume the two-component model for $pp \to pX$ given above. The higher-twist term due to $qq \to p\overline{q}$ produces an isolated proton as a small color singlet which is unaffected by the nuclear environment; in contrast, the protons produced by the standard leading-twist contribution $qq \to qq \to qp(qq)$ with jet fragmentation are absorbed. This immediately explains why the effective power n at fixed x_T increases with increased centrality, consistent with RHIC measurements for charged hadron triggers. See Figure 6.

Furthermore, since the ratio of color-transparent higher-twist contributions to color-opaque leading-twist to the proton production cross section is increased in events with high centrality ($N_{part} > 250$), we can also understand why the number of same side hadrons correlated with a the proton trigger decreases as the number of hadrons produced in the collision increases – the number (solid red squares) of same-side mesons associated with a proton trigger actually decreases even though as N_{part} increases from 250 to 350. See Figure 2. The directly produced proton interacts much less in the nuclear medium than a proton produced via jet fragmentation. In contrast, the meson trigger does not show this effect – the number of same-side mesons (solid blue circles) increase monotonically with N_{part}.

Similar results are also expected for hyperons. For example, a Λ can be produced directly at large transverse momentum via the semi-exclusive subprocess $ud \to \Lambda\ \overline{s}$ in analogy to the $uu \to p\overline{d}$ subprocess illustrated in Figure 8. One can produce antiprotons directly via the hard semi-exclusive process $gg \to \overline{p}\ uud$.

The $pp \to \pi X$ cross section also receives leading-twist fragmentation and direct higher-twist contributions from $gq \to \pi q$, etc.; however, as seen from the power fall-off of $n(x_T)$ shown in Figure 5, higher-twist processes are evidently relatively more significant for proton compared to pion triggers in the RHIC kinematic domain. Thus color transparency and direct hadron production is mostly associated with proton and other baryon triggers.

Clearly careful analyses and measurements at RHIC over a wide range of energies is needed to validate or disprove the connections between higher-twist direct reactions and anomalous heavy ion collision phenomena. Measurements of the associated particles in direct photon production will also be very valuable for understanding these remarkable features of QCD in the nuclear medium.

Acknowledgments:

I thank Anne Sickles, Michael Tannenbaum, and Werner Vogelsang for helpful comments.

References

[1] S. S. Adler *et al.* [PHENIX Collaboration], Phys. Rev. Lett. **91**, 172301 (2003) [arXiv:nucl-ex/0305036].

[2] B. I. Abelev *et al.* [STAR Collaboration], Phys. Lett. B **655**, 104 (2007) [arXiv:nucl-ex/0703040].

[3] A. Adare *et al.* [PHENIX Collaboration], Phys. Lett. B **649**, 359 (2007) [arXiv:nucl-ex/0611016].

[4] A. Sickles, arXiv:0712.0317 [nucl-ex].

[5] S. M. Berman, J. D. Bjorken and J. B. Kogut, Phys. Rev. D **4**, 3388 (1971).

[6] S. J. Brodsky, H. J. Pirner and J. Raufeisen, Phys. Lett. B **637**, 58 (2006) [arXiv:hep-ph/0510315].

[7] J. Cronin in the Proceedings of The SLAC Summer Institute On Particle Physics, July 29 - August 10, 1974.

[8] S. S. Adler *et al.* [PHENIX Collaboration], Phys. Rev. C **69**, 034910 (2004) [arXiv:nucl-ex/0308006].

[9] A. Adare *et al.* [PHENIX Collaboration], Phys. Rev. D **76**, 051106 (2007) [arXiv:0704.3599 [hep-ex]].

[10] M. J. Tannenbaum, PoS C **FRNC2006**, 001 (2006) [arXiv:nucl-ex/0611008].

[11] S. S. Adler *et al.* [PHENIX Collaboration], Phys. Rev. Lett. **98**, 012002 (2007) [arXiv:hep-ex/0609031].

[12] S. J. Brodsky, G. P. Lepage and P. B. Mackenzie, Phys. Rev. D **28**, 228 (1983).

[13] M. Binger and S. J. Brodsky, Phys. Rev. D **74**, 054016 (2006) [arXiv:hep-ph/0602199].

[14] S. J. Brodsky, M. Diehl, P. Hoyer and S. Peigne, Phys. Lett. B **449**, 306 (1999) [arXiv:hep-ph/9812277].

[15] R. Blankenbecler, S. J. Brodsky and J. F. Gunion, Phys. Rev. D **12**, 3469 (1975).

[16] S. J. Brodsky, M. Burkardt and I. Schmidt, Nucl. Phys. B **441**, 197 (1995) [arXiv:hep-ph/9401328].

[17] E. L. Berger and S. J. Brodsky, Phys. Rev. Lett. **42**, 940 (1979).

[18] G. P. Lepage and S. J. Brodsky, Phys. Rev. D **22**, 2157 (1980).

[19] S. J. Brodsky and G. F. de Teramond, arXiv:0709.2072 [hep-ph].

[20] A. V. Efremov and A. V. Radyushkin, Phys. Lett. B **94**, 245 (1980).

[21] D. de Florian, W. Vogelsang and F. Wagner, Phys. Rev. D **76**, 094021 (2007) [arXiv:0708.3060 [hep-ph]].

[22] G. Bertsch, S. J. Brodsky, A. S. Goldhaber and J. F. Gunion, Phys. Rev. Lett. **47**, 297 (1981).

[23] S. J. Brodsky and A. H. Mueller, Phys. Lett. B **206**, 685 (1988).

[24] L. Frankfurt, G. A. Miller and M. Strikman, Comments Nucl. Part. Phys. **21**, 1 (1992).

[25] E. M. Aitala *et al.* [E791 Collaboration], Phys. Rev. Lett. **86**, 4773 (2001) [arXiv:hep-ex/0010044].

[26] B. Clasie *et al.*, Phys. Rev. Lett. **99**, 242502 (2007) [arXiv:0707.1481 [nucl-ex]].

[27] A. S. Carroll *et al.*, Phys. Rev. Lett. **61**, 1698 (1988).

[28] I. Mardor *et al.*, Phys. Rev. Lett. **81**, 5085 (1998).

[29] G. R. Court *et al.*, Phys. Rev. Lett. **57**, 507 (1986).

[30] S. J. Brodsky and G. F. de Teramond, Phys. Rev. Lett. **60**, 1924 (1988).

Particle ratios change with centrality!

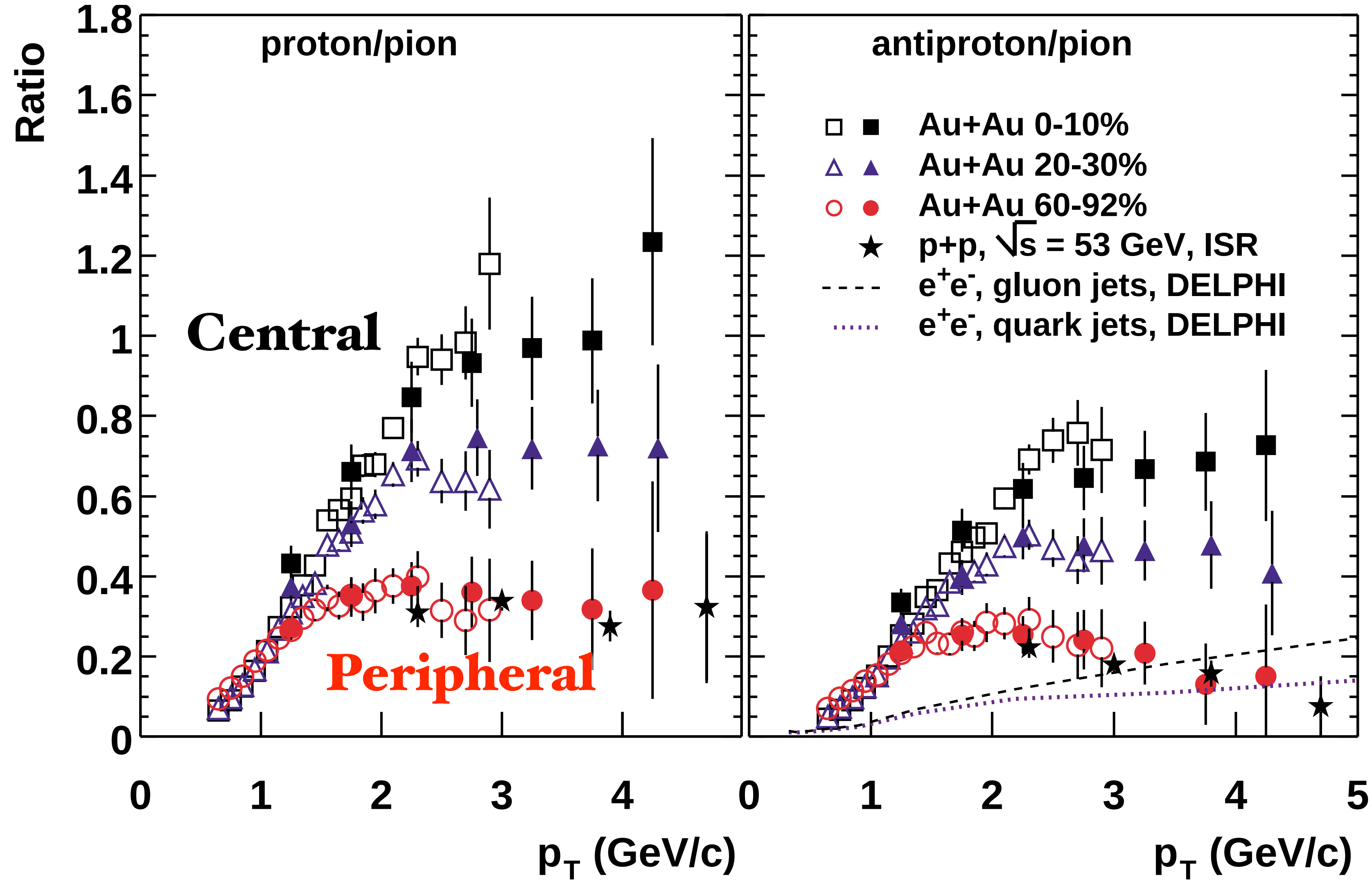

Figure 1. Ratio of proton to pion and antiproton to pion production as a function of p_T for Au-Au collisions at at $\sqrt{s} = 200$ GeV for different centrality. Open and filled symbols represent charged and neutral pions, respectively. The stars show the particle ratio for pp collisions at $\sqrt{s} = 53$ GeV. The ratio for quark and gluon jet fragmentation are also shown. From ref. 1

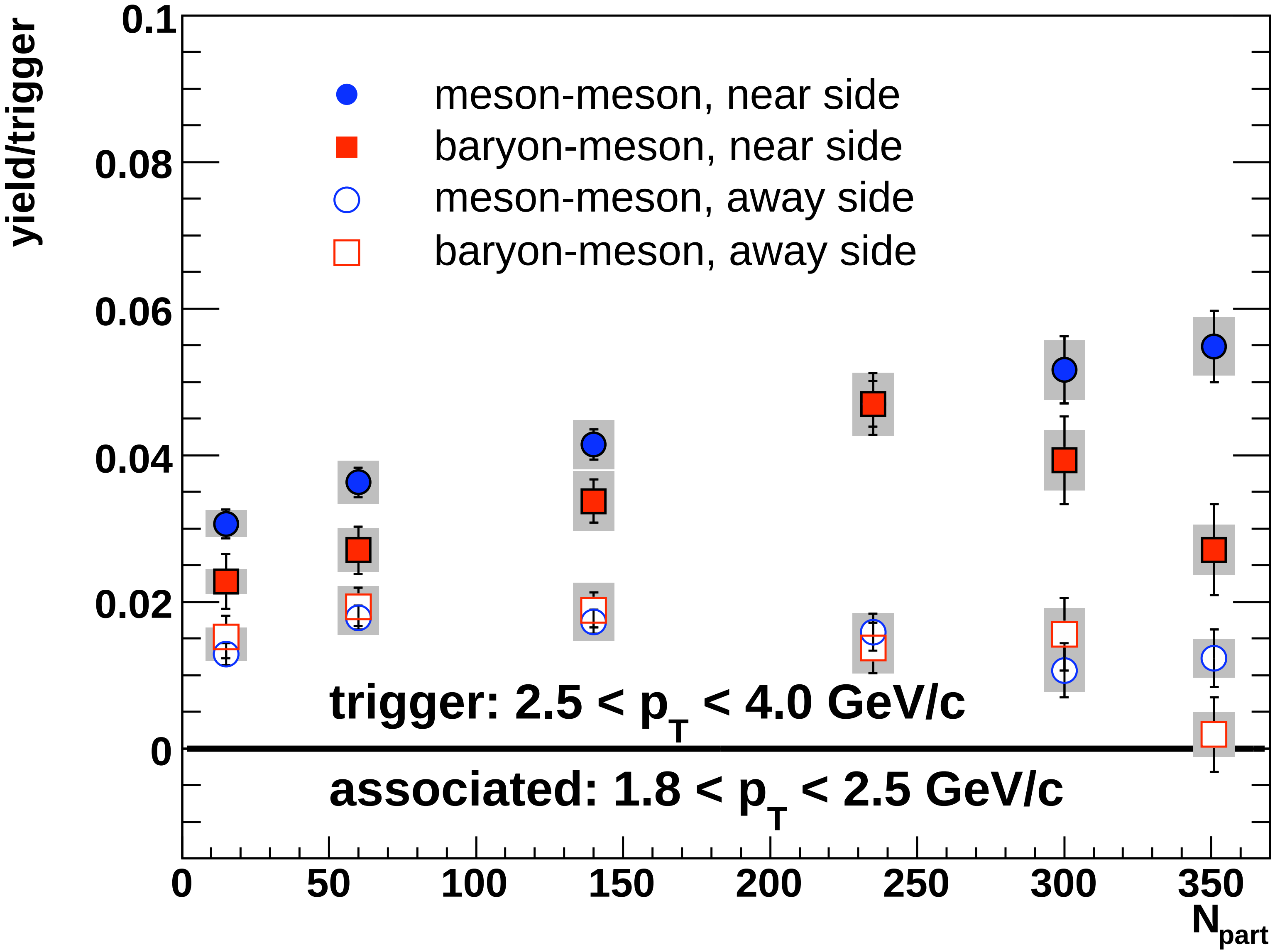

Figure 2. Same-side and away-side correlated hadrons for meson and baryon triggers as a function of the total multiplicity. The number of same-side particles associated with a proton trigger **decreases** as the total number of particles N_{part} produced in the heavy ion collisions increases; i.e., increasing centrality. From ref. 3

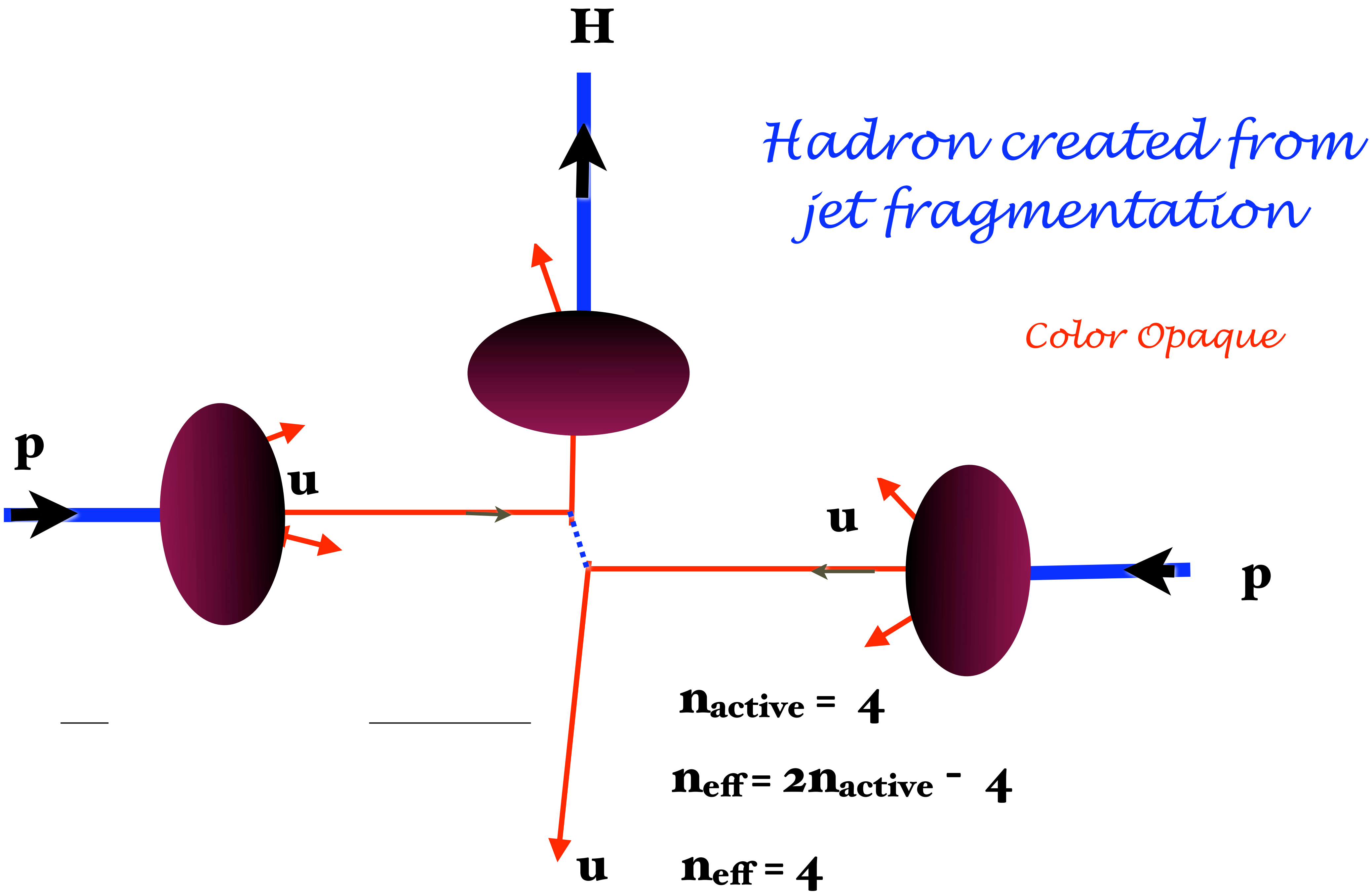

Figure 3. Standard leading-twist quark-quark scattering contribution to hadron production.

QCD prediction: Modification of power fall-off due to DGLAP evolution and the Running Coupling

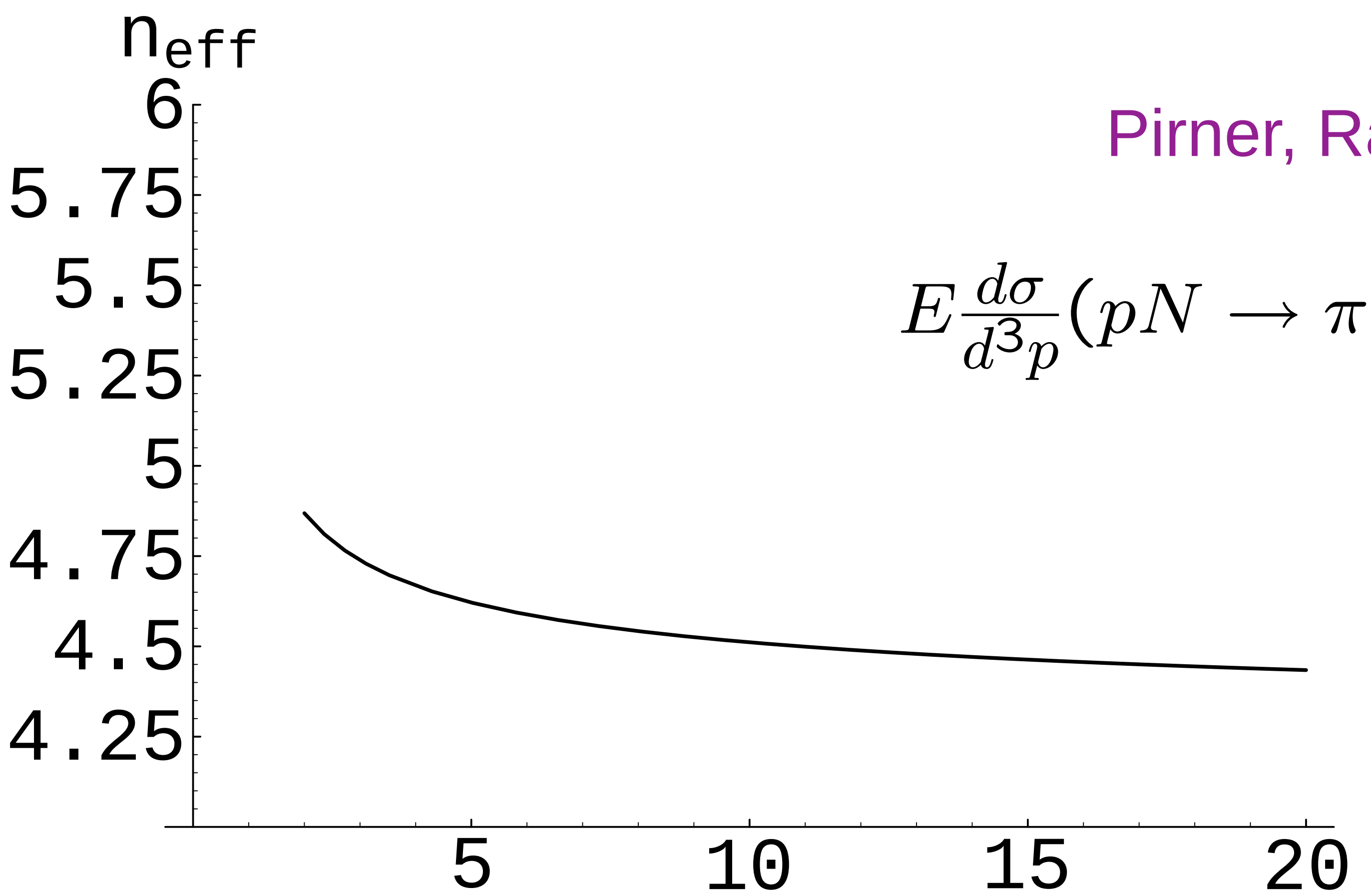

Pirner, Raufeisen, sjb

$$E\frac{d\sigma}{d^3p}(pN \to \pi X) = \frac{F(x_T, \theta_{CM})}{p_T^{n_{eff}}}$$

$n_{eff} \sim 4.5$

Key test of PQCD: power-law fall-off at fixed x_T $\quad x_T = \frac{2p_T}{\sqrt{s}}$

Figure 4. Modification of scale-invariance from the logarithmic running of the QCD coupling constant and DGLAP evolution. From ref. 6.

$$E\frac{d\sigma}{d^3p}(pp \to HX) = \frac{F(x_T, \theta_{cm} = \pi/2)}{p_T^n}$$

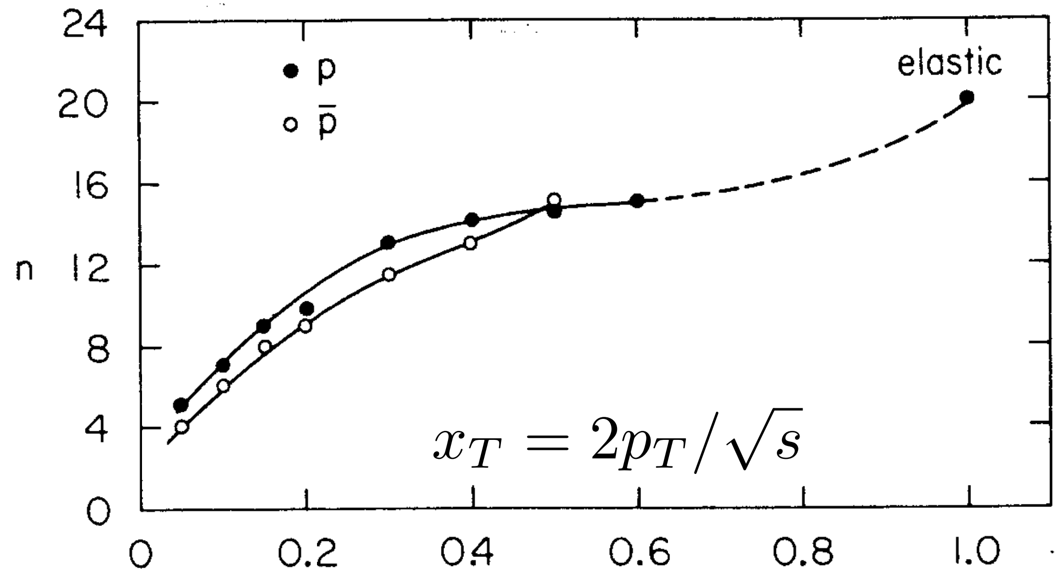

J. W. Cronin, SSI 1974

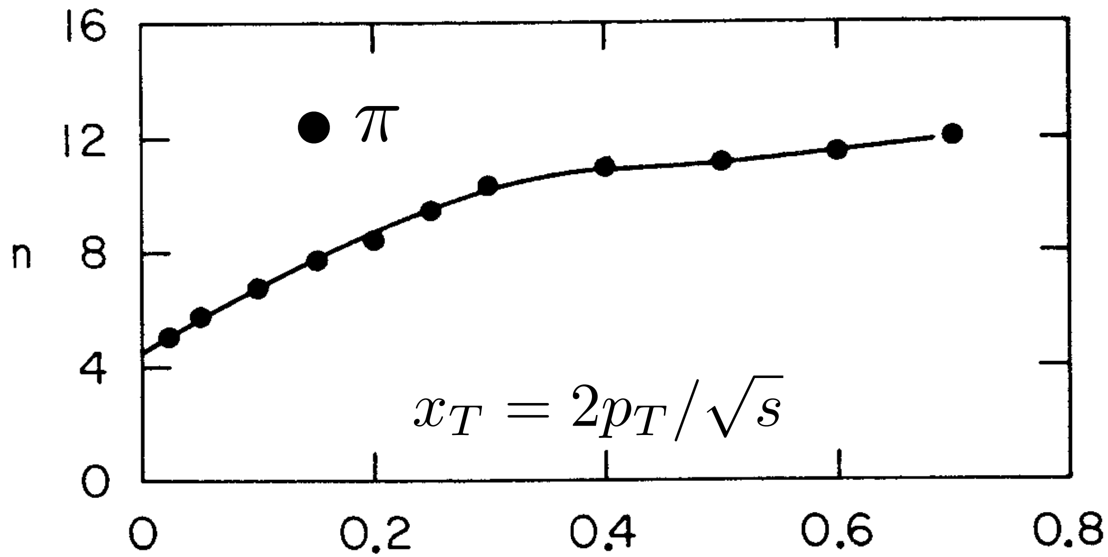

Figure 5. Effective power-law fall-off of the inclusive cross section for proton, antiproton and pion hadroproduction at fixed x_T and fixed θ_{cm}. From ref. 7.

$\sqrt{s_{NN}} = 130$ and 200 GeV

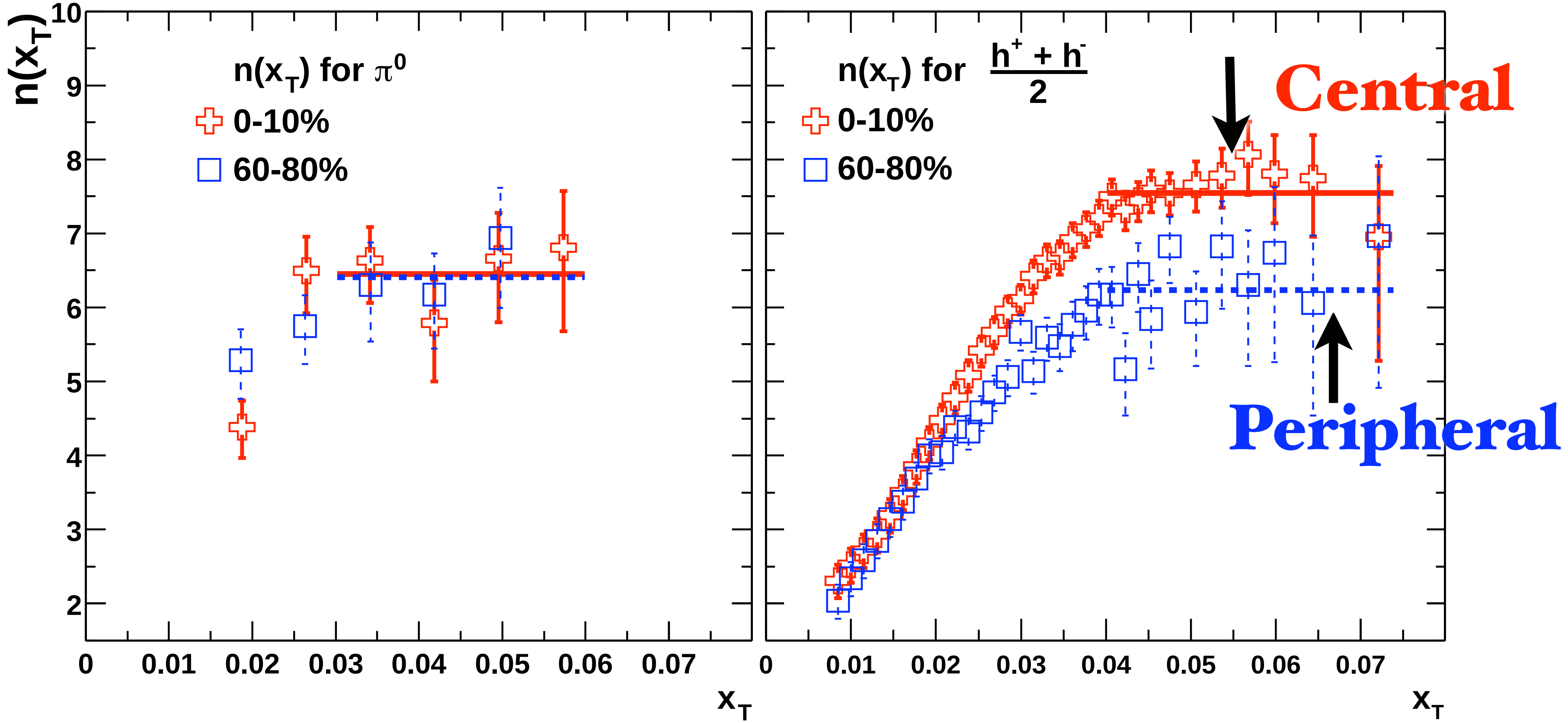

Figure 6. Effective power-law fall-off of the inclusive cross section for π^0 and charged particle hadroproduction at fixed x_T and fixed θ_{cm} at RHIC energies. The power law increases as a function of x_T and is different for central and peripheral collisions in the case of charged particle production. The charged hadrons include protons and antiprotons. From ref. 8.

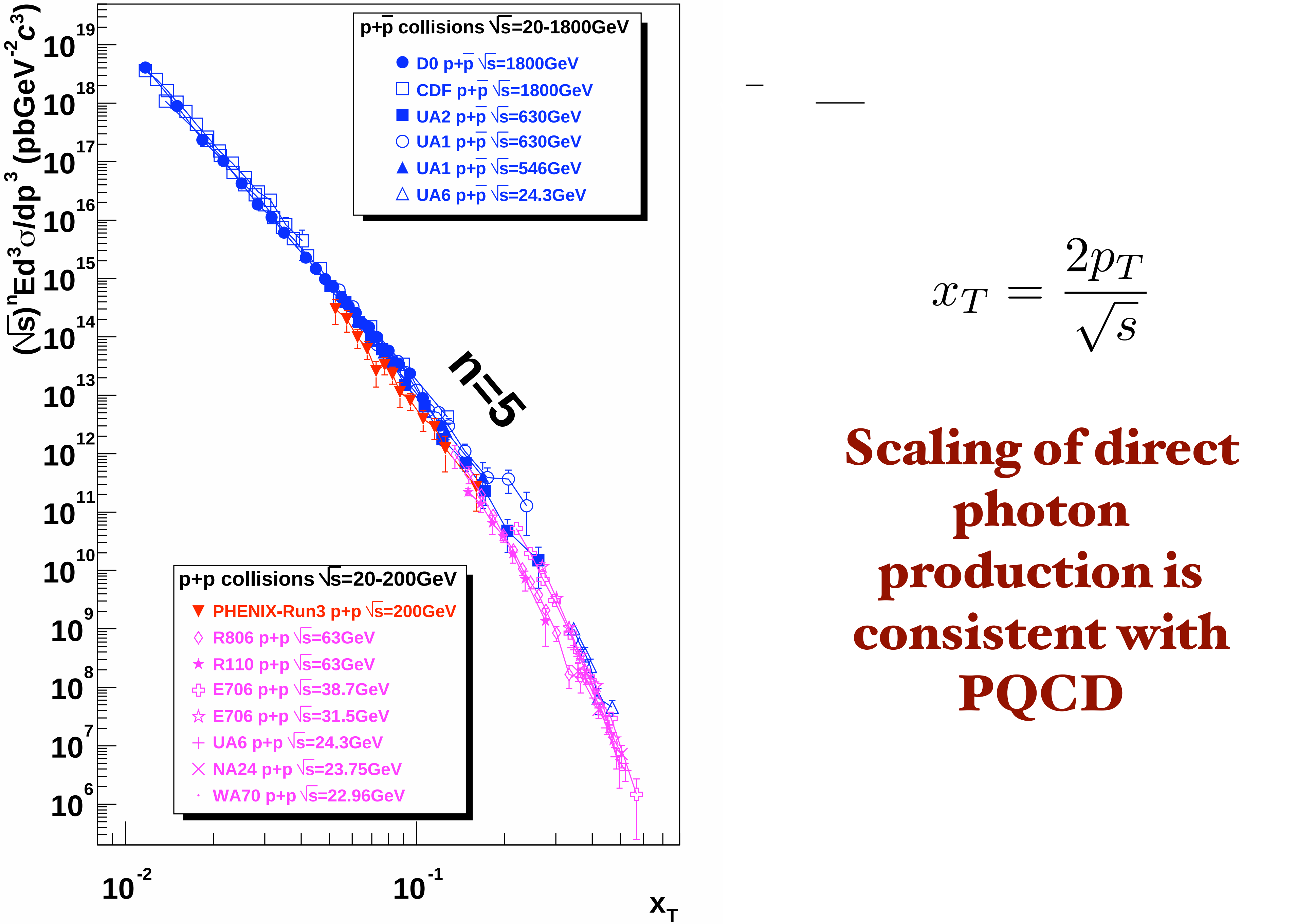

Figure 7. Scaling of the inclusive photon cross section at fixed x_T. From refs. 10, 11.

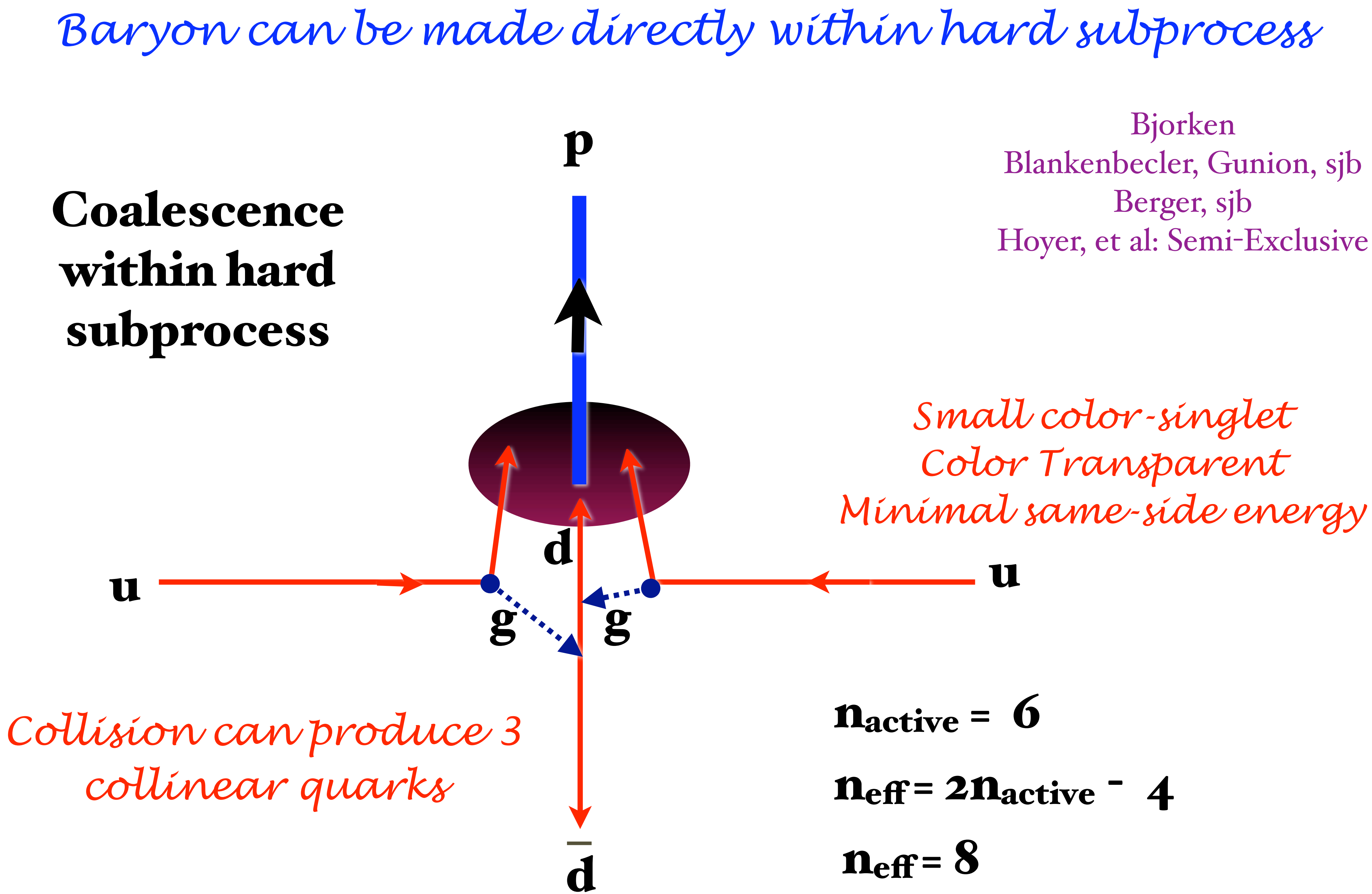

Figure 8. Higher-twist contribution to proton production at high p_T. The proton is produced directly within the 6-parton hard subprocess.